Plant Physiology, August 1999, Vol. 120, pp. 1129–1136, www.plantphysiol.org © 1999 American Society of Plant Physiologists

Characterization of Two Photosynthetic Mutants of Maize[1]

Donald A. Heck, Donald Miles, and Parag R. Chitnis*

Department of Biochemistry, Biophysics and Molecular Biology, Iowa State University, Ames, Iowa, 50011 (D.A.H., P.R.C.); and Division of Biological Sciences, University of Columbia, Columbia, Missouri 65211 (D.M.)

We describe here the biochemical characteristics of the *hcf*44 and *hcf*47 (high chlorophyll fluorescence) mutants of maize (*Zea mays* L.). Both mutants were sensitive to high light intensities, exhibiting reduced growth and fluorescence intensity. Electron transport through the mutants' photosystem (PS) I and PSII reaction centers was reduced and $NADP^+$ photoreduction was absent. Western analysis revealed that the *hcf*44 mutant was missing some or all of the PsaC, PsaD, and PsaE polypeptides of the PSI reaction center, and reverse transcriptase-polymerase chain reaction demonstrated that this loss was the result of a posttranscriptional event. The *hcf*47 mutant had reduced levels of many PSI and PSII polypeptides. These data indicate a possible defect in the synthesis or assembly of the PsaC subunit in the *hcf*44 mutant, whereas the *hcf*47 mutant may have a more general defect in the biogenesis of photosynthetic membranes. Our results demonstrate the coordinated assembly of the peripheral proteins into the PSI complexes of higher plants and demonstrate the in vivo requirement of PsaC, PsaD, and PsaE subunits for the function of PSI in higher plants.

Oxygenic photosynthesis involves the harvesting of light energy and its conversion into chemical energy within the thylakoid membranes of chloroplasts and in cyanobacteria. Photosynthetic electron transport utilizes four membrane complexes: PSII, Cyt b_6/f, PSI, and ATP synthase. Electrons from the light-driven oxidation of water within PSII are transferred to PSI through the Cyt b_6/f complex and two soluble electron carriers, plastoquinone and plastocyanin. PSI functions as a plastocyanin-Fd oxidoreductase that generates reducing power and NADPH. Photosynthetic electron transport produces a proton gradient across the thylakoid membrane that is used to drive the production of ATP via ATP synthase.

Photosynthetic mutants of cyanobacteria and green algae have been used extensively to study the biogenesis and function of photosynthetic complexes (Pakrasi, 1995; Chitnis, 1998; Hippler et al., 1998; Sun et al., 1998). The study of photosynthetic mutants in plants has been limited, since many defects in photosynthesis are lethal. One class of mutants in maize (*Zea mays L.*), *hcf* (high chlorophyll fluorescence), has been useful in providing clues about the organization, function, and biogenesis of specific membrane complexes within the thylakoid membranes of higher plants. These seedling-lethal mutants are defective in electron flow through the photosynthetic complexes. Any limitations in photosynthetic electron transport result in the increased loss of absorbed light through fluorescence. The first *hcf* mutants were isolated in 1972 (Miles and Daniel, 1974), and over 100 mutants have been isolated since then (Miles, 1994).

Many *hcf* mutants of maize contain lesions that affect PSI activity, providing an opportunity to study PSI assembly and function in a eukaryotic photosynthetic organism. The *hcf*43, *hcf*49, *hcf*104, and *hcf*122 mutants exhibit a general loss of the PsaA-PsaB core subunits in addition to other PSI subunits (Barkan et al., 1986; Miles, 1994). The *hcf*50 mutant affects the PSI complex most severely. This mutant has lost the PSI core complex entirely, but this does not affect the other photosystem components (Miles, 1994; M.J. Hitchler, D.A. Heck, and P.R. Chitnis, unpublished observations). The *hcf*38 mutant has a reduction in the PsaA-PsaB core subunits, which is accompanied by a decrease in the amount of PsaA-PsaB mRNA. Also, other chloroplast mRNAs are reduced in amount or absent, suggesting a lesion in a nuclear gene that regulates chloroplast mRNA processing (Barkan et al., 1986). In contrast to the other *hcf* mutants, *hcf*101 has a 5-fold increase in the rate of PSI electron transport, suggesting a loss of regulatory control of electron transport from plastocyanin to the P700 reaction center (Miles, 1994).

The *hcf*44 and *hcf*47 mutants represent two nuclear mutations that have been mapped to chromosomes 1 and 10, respectively (Miles et al., 1985). These mutants have been identified previously as having a photosynthetic block beyond the PSII reaction center, possibly within the PSI reaction center for the *hcf*44 mutant and within the Cyt b_6/f complex for the *hcf*47 mutant (Miles, 1994; Neuffer et al., 1997). We report here the detailed characterization of the maize *hcf*44 and *hcf*47 mutants. The *hcf*44 mutant may be defective in the stable assembly of the PsaC subunit into the PSI core complex, whereas the *hcf*47 mutant may have a more general defect within the photosynthetic membranes.

MATERIALS AND METHODS

Maize Stocks and Other Materials

A series of ethyl-methanesulfonate-induced mutants were generated by M.G. Neuffer (University of Missouri,

[1] This work was supported partially by the U.S. Department of Agriculture-National Research Initiative Competitive Grants Program (grant no. 97–35306–4555) and the National Science Foundation (grant no. MCB9723001). This is journal paper no. J–18286 of the Iowa Agriculture and Home Economics Experiment Station, Ames, project nos. 3,416 and 3,496, and was supported by the Hatch Act and by State of Iowa funds.

* Corresponding author; e-mail chitnis@iastate.edu; fax 515–294–0453.

Abbreviation: RT, reverse transcriptase.

Columbia) and screened for *hcf* mutants (Miles and Daniel, 1974). Rabbit-derived antibodies for PsaA-PsaB were obtained previously (Sun et al., 1998). Additional antibodies were generous gifts of John Golbeck (Pennsylvania State University, University Park) (PsaC, PsaD, and PsaE), Elena Zak and Himadri Pakrasi (Washington University, St. Louis) (BtpA and D1-D2), Bridgette Barry and Charles Youcum (University of Minnesota, St. Paul) (PsbO), and James Guikema (Kansas State University, Manhattan) (LHCI). The antibodies derived for the core complex subunits in PSI recognize both PsaA and PsaB, and the antibodies derived for the core complex subunits in PSII recognize both D1 and D2.

Isolation of Photosynthetic Membranes

Maize (*Zea mays* L.) seedlings were grown under medium-intensity light (approximately 200 μmol m^{-2} s^{-1}) with 16-h days unless otherwise noted. Seedling leaves (approximately 1 g) were harvested and disrupted with a pestle and mortar in STN buffer (0.8 M Suc, 10 mM NaCl, 20 mM Tricine, 5 mM $MgCl_2$, and 1 mg BSA L^{-1}). Disrupted tissue was then passed through four layers of Miracloth (Calbiochem), centrifuged at 200*g* to remove additional cellular debris, and then centrifuged at 25,000*g* for 25 min to obtain a crude membrane pellet. The membrane pellet was then resuspended in STN buffer without BSA and stored at −20°C until used. The total membrane chlorophyll concentration and chlorophyll *a/b* ratio were determined in 80% (v/v) acetone by the method described in Hipkins and Baker (1986).

Fluorescence Induction Measurements

Wild-type and mutant seedlings were grown under high-intensity (335 μmol m^{-2} s^{-1}), medium-intensity (180 μmol m^{-2} s^{-1}), or low-intensity (8.75 μmol m^{-2} s^{-1}) light. Fluorescence induction was measured using a kinetic fluorescence CCD camera (Photon Systems Instruments, Brno, Czech Republic) that uses far-red (735 nm) LEDs to generate approximately 400 μmol m^{-2} s^{-1} of light. Measurements were taken using the first leaf upon emergence and the second leaf thereafter; fluorescence was measured as the average of the whole leaf. Fluorescence was not significantly different when measured from different leaves of the same plant at the same stage of development (data not shown). Fluorescence data were gathered every 2 or 3 d from the point of emergence through the four- or five-leaf stage or until seedling death in the case of mutant plants.

Measurement of Photosynthetic Electron Transport

Rates of oxygen evolution or uptake were determined with an oxygen electrode (Hansatech, King's Lynn, UK) at 25°C and a light intensity of 2,430 μmol m^{-2} s^{-1} for oxygen evolution and at 18,300 μmol m^{-2} s^{-1} for oxygen uptake in a 1-mL reaction volume. The rate of oxygen evolution by PSII was determined with membrane homogenate containing 30 or 60 μg of chlorophyll per sample with 3 mM $K_3Fe(CN)_6$ and 40 μM *p*-phenylenediamine. The rate of oxygen uptake by PSI according to the Hill reactions (Trebst, 1972) was determined with 5 or 10 μg of chlorophyll per sample in the presence of 50 μM DCMU, 2 mM methyl viologen, 1 mM 3,6-diaminodurene, and 1 mM ascorbic acid. These values were then converted to the rate of oxygen evolution or consumption per milligram of tissue using the total chlorophyll concentration data from Table I, and expressed as a percent of control. Statistical significance was determined with a nonpaired, two-tailed Student's *t* test.

Rates of Fd-mediated $NADP^+$ photoreduction were measured as the rate of change in the absorption of NADPH at 340 nm. We found measurements to be consistent when using Cyt c_6 as an artificial electron donor. Reductase activity was determined in a 700-μL volume using membrane homogenate containing 7 μg of chlorophyll. Reactions were performed in the presence of 0.8 mM $NADP^+$, 5 μM Fd, 0.8 μM Fd-$NADP^+$ reductase, 2.5 mM Cyt c_6, 50 mM Tricine, 10 mM $MgCl_2$, 0.1% (v/v) β-mercaptoethanol, 6 mM sodium ascorbate, and 0.05% (w/v) *n*-dodecyl β-maltoside. The rates were determined using a spectrophotometer (model UV160U, Shimadzu, Columbia, MD) fitted with a narrow-band interference filter attached to the surface of the photomultiplier. The sample was illuminated using high-intensity LEDs (LS1, Hansatech). The light intensity was saturating at the chlorophyll concentrations used.

Analytical Gel Electrophoresis and Immunodetection

Whole membrane preparations were denatured at 37°C for 1 h in 40% (w/v) glycerol, 10% (w/v) SDS, 9.3% (w/v) DTT, and bromphenol blue dye in upper reservoir buffer. Samples were fractionated by SDS-PAGE using a running

Table I. *Primer pairs used for RT-PCR and optimal annealing temperature*

Forward and reverse primers are listed in the 5′ to 3′ direction with their optimal annealing temperature (T_A).

Fragment	Forward Primer	Reverse Primer	T_A
			°C
psaC	TCATTGTGTACGAGCTTGCC	AAGATAGAGCCATGCTGCG	58
psaD	TCATTGTGTACGAGCTTGCC	AAGATAGAGCCATGCTGCG	60
psaE	AGTCCTACTGGTACAACGG	CGTAGTTGTTGGTCGACAC	51
actin	TGGCATTGTCAACAACTGG	TCATTAGGTGGTCGGTGAGG	53

gel containing 14% (w/v) acrylamide and 6 M urea with an upper reservoir buffer of 1.0 M Tris, 1.0 M Tricine, and 1.0% (w/v) SDS (pH approximately 8.2) and a lower reservoir buffer of 2 M Tris (pH 8.9) (Xu et al., 1994). For visual inspection, gels were silver-stained or stained with Coomassie Blue. For immunodetection, proteins were electrotransferred to PVDF membranes (Immobilon-P, Millipore), and the antibody-antigen interaction was detected by enhanced chemiluminescence (Amersham).

RNA Analysis by RT-PCR

Total RNA was isolated using the phenol-SDS method (Ausubel et al., 1988). Leaf tissue (approximately 200 mg) was disrupted with a mortar and pestle in liquid nitrogen. The tissue was then added to a warm emulsion (65°C) of 10 mL of phenol plus 12 mL of extraction buffer (100 mM Tris, pH 8.0, 50 mM EDTA, pH 8.0, 500 mM NaCl, 10 mM β-mercaptoethanol, and 0.4% [w/v] SDS). Tissue was stirred in emulsion for 5 min, after which time 10 mL of chloroform:isoamylalcohol (24:1) was added and stirred for another 5 min. The suspension was centrifuged at 12,000*g* for 10 min at room temperature. The aqueous phase was collected and transferred to a new tube with 10 mL of chloroform:isoamylalcohol (24:1), mixed, and centrifuged again at 12,000*g* for 10 min. The aqueous phase was again taken and adjusted to 2 M ammonium acetate and precipitated with 1 volume of isopropanol. RNA was pelleted at 12,000*g* for 15 min and resuspended in RNase-free water.

Total RNA was reverse-transcribed into cDNA using random hexamer reverse transcription of RNA with a PCR kit (GeneAmp, Perkin-Elmer). PCR amplification of PsaC, PsaD, PsaE, and actin target cDNAs using the primer pairs shown in Table I was optimized for the proper amount of cDNA template to be added and the number of PCR cycles to be performed according to the method of Gause and Adamovicz (1995). PCR amplification of target cDNAs from wild-type and mutant seedling RNA was then performed within the linear range of product amplification. PCR products were transferred to nylon membranes by Southern blotting for hybridizing with ^{32}P-labeled probes. Probe DNA was generated by PCR using primer pairs to obtain PsaC, PsaD, PsaE, and actin fragments from maize genomic DNA. Probe DNA was labeled with a random-primer labeling kit (Decaprime, Ambion, Austin, TX), using [α-^{32}P]dCTP (ICN).

RESULTS

Leaf Fluorescence of Mutants Is Sustained at Peak Levels

Variable fluorescence is a simple and reliable measure of photosynthetic activity in maize. Using a kinetic fluorescence camera, whole-leaf fluorescence of wild-type and mutant *hcf* seedlings was recorded (Fig. 1), and is representative of both *hcf*44 and *hcf*47 wild-type and mutant seedlings. Wild-type seedlings exhibit a typical pattern of fluorescence marked by a fluorescence peak (F_p) that is followed by a slow decline in fluorescence to a semi steady-state (F_s). This slow decline in fluorescence is due to normal

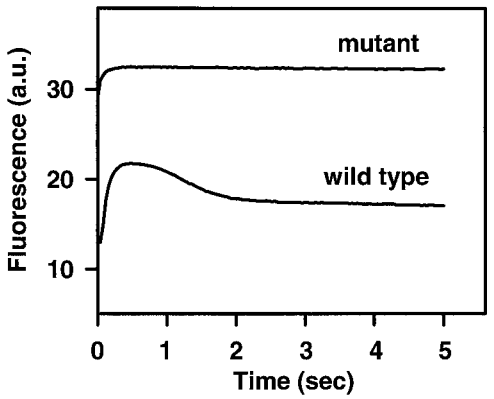

Figure 1. Fluorescence measurements of *hcf*44 and *hcf*47 seedlings. Wild-type and mutant seedlings were grown under high-intensity (335 μmol m^{-2} s^{-1}), medium-intensity (180 μmol m^{-2} s^{-1}), or low-intensity (8.75 μmol m^{-2} s^{-1}) light conditions and used for fluorescence induction measurements. The graph qualitatively represents both *hcf*44 and *hcf*47 mutant (top line) and wild-type (bottom line) seedlings grown under all three light conditions. A quantitative assessment of peak fluorescence for wild-type and mutant seedlings grown under high, medium, or low light intensity is presented in Figure 2.

electron transport on the reducing side of PSI (Miles, 1980). In contrast, fluorescence is sustained at peak levels in the mutant seedlings, which is consistent with the notion that these mutants are unable to perform electron transport through PSI.

Because photochemical quenching of light energy does not occur in the mutants, we wanted to measure the effects of different light intensities on seedling growth and viability. We examined the fluorescence of seedlings subjected to high-intensity (335 μmol m^{-2} s^{-1}), medium-intensity (180 μmol m^{-2} s^{-1}), or low-intensity (8.75 μmol m^{-2} s^{-1}) light (Fig. 2). Wild-type plants grown under high light had reduced growth compared with the other wild-type plants but otherwise appeared normal. Mutant plants grown under high light were pale yellow and dying, whereas the mutant plants grown under medium and low light were light green and more vigorous. This pattern of growth was similar between the two lines, however, the mutant *hcf*47 plants exhibited a more severe phenotype (data not shown).

The fluorescence pattern was unchanged for the wild-type and mutant seedlings under all conditions of light; however, F_p varied for the mutant seedlings under different light intensities (Fig. 2). For the *hcf*44 mutant seedlings, F_p was significantly greater for seedlings that had been grown under medium and low light intensities ($P < 0.0001$) (Fig. 2a). Mutant seedlings grown under low light intensity had a F_p of 42.9 $\pm$ 2.1 arbitrary units, which is approximately 2-fold greater than that in the wild-type seedlings. Mutant seedlings grown under high-intensity light had peak fluorescence measurements similar to those of wild-type seedlings. For the *hcf*47 mutant seedlings, F_p was also significantly increased in seedlings grown under medium and low light intensities ($P < 0.0001$) (Fig. 2b). Interestingly, mutant seedlings grown under high light intensity

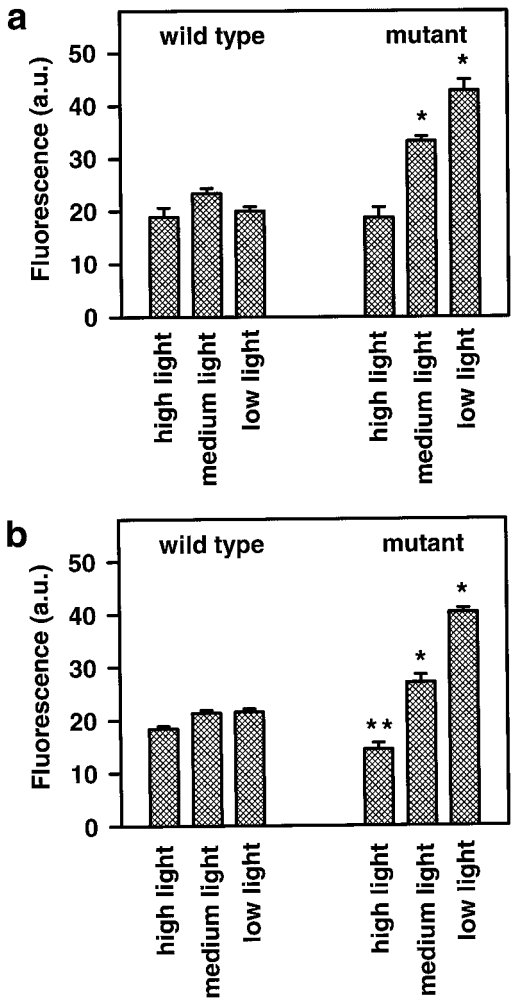

Figure 2. Peak fluorescence for wild-type and mutant seedlings grown under high, medium, and low light intensity and measured for peak fluorescence (using arbitrary units [a.u.]) at different stages of development. a, Average peak fluorescence for wild-type and mutant *hcf*44 seedlings; b, average peak fluorescence for wild-type and mutant *hcf*47 seedlings. Each bar represents the average ± SE of four to 44 independent measurements. Statistical significance was determined using a two-tailed, nonpaired Student's *t* test. *, $P < 0.0001$; **, $P < 0.01$.

had peak fluorescence measurements that were slightly but significantly reduced from those of wild-type seedlings ($P < 0.01$).

Mutants Contain Reduced Chlorophyll Concentrations

Visibly, the *hcf*44 and *hcf*47 mutants were pale-green to yellow-green in color. Chlorophyll analysis of seedlings grown at medium light intensity shows a significant reduction in total chlorophyll content per milligram of tissue for both the *hcf*44 and *hcf*47 mutants compared with wild-type seedlings ($P < 0.001$) (Table II). Field-grown mutant seedlings under full sun had chlorophyll concentrations less than 10% of their wild-type siblings (data not shown). The chlorophyll *a/b* ratio for both mutant seedlings was also significantly reduced ($P < 0.01$), suggesting a greater loss of PSI reaction centers, which contain predominantly chlorophyll *a*.

PSI and PSII Reaction Center Activities Are Reduced in the Mutants

To determine the integrity of the PSI and PSII reaction centers, reaction center functionality was tested individually according to the Hill reactions describing oxygen evolution (PSII) and oxygen uptake (PSI) (Table III) (Trebst, 1972; Hipkins and Baker, 1986). PSII function was measured as the rate of oxygen evolution using *p*-phenylenediamine as the electron donor and potassium ferricyanide as the electron acceptor. Using membrane homogenates containing equal amounts of chlorophyll, oxygen evolution for the mutant *hcf*44 seedlings was not significantly different than that observed for the wild-type seedlings. However, since the chlorophyll content per milligram of leaf tissue for the mutant seedlings was only 35% of wild-type seedlings (when calculated on an equal-tissue basis), oxygen evolution for the mutant seedlings was only 45% of control (Table III). Oxygen evolution measured from membrane homogenates of the mutant *hcf*47 seedling was only 6.0 ± 3.0 μmol O_2 mg^{-1} chlorophyll h^{-1}, significantly less than that of the wild-type seedlings ($P < 0.001$). On an equal-tissue basis, this translates to a rate of oxygen evolution for mutant seedlings of only 5% of control (Table III).

The function of PSI reaction centers was measured as the rate of oxygen uptake using 3,6-diaminodurene and ascorbate as electron donors and methyl viologen as the electron acceptor. Using membrane homogenates containing equal amounts of chlorophyll, the rate of oxygen uptake for both *hcf*44 and *hcf*47 mutant seedlings was similar to the rate of oxygen uptake for the wild-type seedlings. On an equal-tissue basis, this translates to a rate of oxygen uptake that was 44% of wild-type seedlings for the *hcf*44 mutants and 14% of wild-type seedlings for the *hcf*47 mutants (Table III). The reductase activity of PSI was measured by determining the rate of $NADP^+$ photoreduction with Fd-$NADP^+$ oxidoreductase mediated through Fd. The rates obtained for wild-type membrane homogenates were comparable to

Table II. *Total chlorophyll content and chlorophyll a/b ratio for hcf44 and hcf47 wild-type and mutant seedlings*

Total chlorophyll content and chlorophyll *a/b* ratios were determined for wild-type and mutant seedlings grown under medium light intensity. Total chlorophyll content of mutant seedlings is also expressed as a percentage of the chlorophyll content for wild-type seedlings. Statistical significance was determined using a two-tailed, nonpaired Student's *t* test (*, $P < 0.001$; **, $P < 0.01$).

Phenotype	Total Chlorophyll	Percentage of Control	Chlorophyll *a/b* Ratio	*n*
	μg/mg tissue			
*hcf*44				
Wild type	2.78 ± 0.13	100	3.92 ± 0.07	5
Mutant	0.96 ± 0.17*	35	2.85 ± 0.15**	4
*hcf*47				
Wild type	2.64 ± 0.25	100	3.65 ± 0.10	5
Mutant	0.42 ± 0.08*	16	2.64 ± 0.22**	3

Table III. *Rates of oxygen evolution (PSII) and uptake (PSI) for hcf44 and hcf47 wild-type and mutant seedlings*

The rates of oxygen evolution and consumption per milligram of chlorophyll were obtained using tissue homogenate containing 30 μg of chlorophyll for oxygen evolution and 5 μg of chlorophyll for oxygen uptake. These values were then converted to the amount of oxygen evolved or consumed per milligram of tissue using the data from Table II and expressed as a percentage of wild-type membrane homogenate (control). Statistical significance was determined using a two-tailed, nonpaired Student's *t* test (*, $P < 0.001$; **, $P < 0.05$; ***, $P = 0.07$ with 2 d.f.).

Phenotype	O_2 Evolution			*n*	O_2 Uptake			*n*
	O_2 evolved	O_2 evolved	Percentage of control[a]		O_2 consumed		Percentage of control[a]	
	μmol O_2 mg^{-1} chlorophyll h^{-1}	*nmol O_2 mg^{-1} tissue h^{-1}*			*μmol O_2 mg^{-1} chlorophyll h^{-1}*	*nmol O_2 mg^{-1} tissue h^{-1}*		
*hcf*44								
Wild type	20.3 ± 3.0	56 ± 8	100	5	154 ± 13	427 ± 37	100	4
Mutant	28.3 ± 6.0	27 ± 6**	49	3	169 ± 22	162 ± 21*	44	4
*hcf*47								
Wild type	24.2 ± 1.5	64 ± 4	100	5	127 ± 30	335 ± 79	100	2
Mutant	6.0 ± 3.0*	3 ± 1*	4	4	114 ± 9	48 ± 4***	14	2

[a] Based on O_2 evolved or consumed per milligram of tissue.

previously published rates for maize thylakoids (He and Malkin, 1992). We could not detect $NADP^+$ photoreduction activity when mutant *hcf*44 or *hcf*47 membranes were used in the assay (Table IV).

The *hcf*44 and *hcf*47 Mutants Are Missing PSI and PSII Reaction Center Subunits

We used western analysis to examine the relative abundance of some of the major proteins of PSI and PSII (Fig. 3). Western analysis of *hcf*44 mutant membranes (Fig. 3, lane 2) showed that the PsaA-PsaB proteins accumulated to the same level as the wild type (Fig. 3, lane 1), whereas the PsaD subunit was in reduced amounts and the PsaC and PsaE subunits were missing entirely. In contrast, the LHCI complex and the two PSII polypeptide subunits, D1-D2 and PsbO, were present at similar levels in the mutant and wild-type membranes. The *hcf*47 mutant membranes exhibited a more general deficiency in photosystem subunit composition, which is consistent with the greater loss of electron transport observed for this mutant shown in Table III. The mutant membranes (Fig. 3, lane 4) had reduced amounts of the PsaA-PsaB proteins and were lacking PsaC,

Table IV. *Rate of $NADP^+$ photoreduction in wild-type and mutant hcf44 and hcf47 seedlings*

The rate of $NADP^+$ photoreduction was determined for wild-type and mutant seedlings grown under medium light intensity. Membrane homogenate containing 7 μg of chlorophyll per sample was used for each determination.

Phenotype	$NADP^+$ Reduction	Percentage of Control	*n*
	μmol NADPH mg^{-1} chlorophyll h^{-1}		
*hcf*44			
Wild type	13.6 ± 1.9	100	4
Mutant	0	0	3
*hcf*47			
Wild type	9.3 ± 1.0	100	4
Mutant	0	0	5

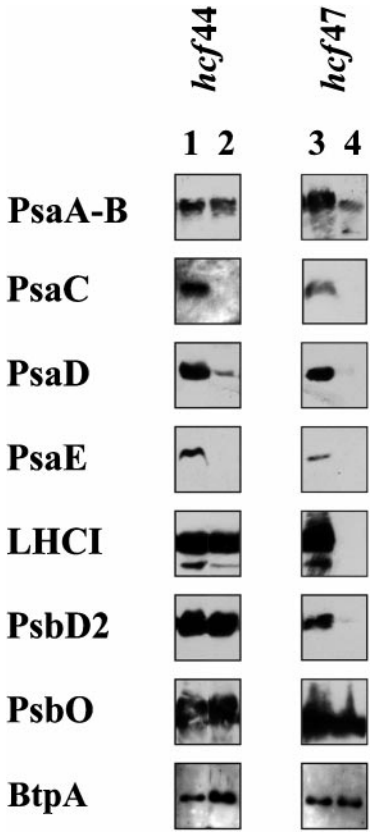

Figure 3. Western analysis of PSI and PSII polypeptides. Membrane homogenates from wild-type or mutant *hcf*44 and *hcf*47 seedlings containing equal amounts of chlorophyll (5 or 10 μg) were electrophoresed using SDS-PAGE. Samples were then electroblotted onto PVDF membranes for immunodetection. Lanes 1 and 3 contain wild-type samples and lanes 2 and 4 contain mutant samples. The figure is representative of two or three determinations per antibody.

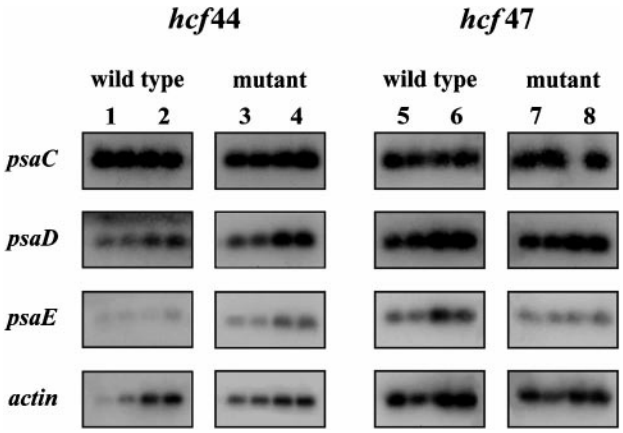

Figure 4. Determination of mRNA levels for the PsaC, PsaD, and PsaE polypeptide subunits using RT-PCR. Total RNA (3 μg) from wild-type and mutant *hcf*44 and *hcf*47 seedlings was isolated for reverse transcription of mRNA transcripts. Resultant cDNA was then used for PCR using the maize actin gene as an internal control. Southern analysis was performed using ^{32}P-labeled probes. For the PCR reaction, lanes 1, 3, 5, and 7 were loaded with 0.5 μL of cDNA sample in duplicate, and lanes 2, 4, 6, and 8 were loaded with 1.0 μL of cDNA sample in duplicate. Lanes 1 and 2 are to be compared with lanes 3 and 4, and lanes 5 and 6 are to be compared to lanes 7 and 8. The actin gene was used as a positive control. Each figure is representative of two independent determinations.

PsaD, PsaE, and LHCI proteins compared with wild type (Fig. 3, lane 3). In addition, the PSII subunits D1-D2 and PsbO were present in reduced amounts (Fig. 3). BtpA, a novel protein involved in the stable assembly of PSI (Bartsevich and Pakrasi, 1997), was increased in the *hcf*44 membranes and unchanged in *hcf*47 membranes.

Figure 3 shows that the *hcf*44 and *hcf*47 mutants were missing (or nearly missing) the PsaC, PsaD, and PsaE subunits. We wanted to determine whether the loss of these subunits was occurring through a loss of transcription or through a posttranscriptional event. RT-PCR was used to determine if the level of mRNA for these subunits was different in the mutant seedlings (Fig. 4). Equal amounts of total RNA were reverse-transcribed and used for PCR amplification using 0.5 μL of cDNA (Fig. 4, lanes 1, 3, 5, and 7) or 1 μL of cDNA (Fig. 4, lanes 2, 4, 6, and 8) in duplicate. Using the maize actin gene to control for sample variability, no significant loss of mRNA occurred in any of the genes tested, and an increase in mRNA from the *psaD* and *psaE* genes may have occurred for the *hcf*44 mutant. These results suggest that the loss of the PsaC, PsaD, and PsaE subunits occurred at a posttranscriptional step, perhaps at the level of translation, protein targeting, or protein stability.

DISCUSSION

The biosynthesis and maintenance of the PSI complex encompasses the coordination of various processes with the potential for many levels of regulation. Assembly involves the expression of chloroplast and nuclear genes, the targeting of subunits to their proper locations within the chloroplast, and the proper organization and assembly of the subunits and cofactors into functional complexes (Boudreau et al., 1997). A disruption at any one of these stages can have a detrimental effect on the whole organism. The evaluation of the functional activities and subunit composition of the maize photosynthetic mutants *hcf*44 and *hcf*47 presented here allows for a more definitive postulation of the defective nature of these mutants.

The rate of oxygen uptake for the *hcf*47 mutant seedlings was similar to that of the wild-type seedlings when measured with equal amounts of chlorophyll. Given the reduced abundance of the PsaA-PsaB core subunits, this may either reflect a limiting factor in our assay for oxygen uptake or the existence of a functional reserve of PSI core complexes. Full activity in the presence of reduced PsaA-PsaB core subunits has been observed before with the *hcf*2 and *hcf*38 mutants of maize (Barkan et al., 1986). The rate of oxygen evolution for the *hcf*47 mutant seedlings was significantly less than wild type when using equal amounts of chlorophyll. When calculated for equal amounts of tissue, PSII activity was only 5% of wild type. Western analysis showed that the hcf47 mutant was missing or nearly missing every photosystem subunit tested, including the PSII subunits D1-D2 and PsbO. With the reduction of these subunits, the PSII complex had no functional reserve like that of the PSI complex. Western analysis also showed equal amounts of BtpA protein when samples were loaded with equal amounts of chlorophyll. When compared on an equal-tissue basis, this would represent about a 7-fold reduction in the amount of BtpA in the mutant seedlings. It is not known, however, whether this loss of BtpA is directly responsible for the loss of PSI subunits, as other photosystem subunits are missing as well.

These observations demonstrate that the *hcf*47 mutants have a more general defect in chloroplast membrane structure, suggesting a possible disruption in protein assembly or targeting to the thylakoid membrane. Protein targeting consists of a small number of highly conserved pathways: SecA-dependent translocation, SRP (signal recognition particle) protein-facilitated targeting, and a pathway dependent on the proton concentration difference across the thylakoid membrane (Δ-pH). The maize genes have been cloned and characterized for two of these pathways, *hcf*106 (Settles et al., 1997) and *tha1* (Voelker and Barkan, 1995). Both mutations result in the loss of photosynthetic complexes by disrupting either the Δ-pH pathway (*hcf*106) or the SecA-dependent pathway (*tha1*) of protein targeting. Specifically, the PsaA, PsaD, PsaF, and D2 in addition to other photosystem subunits are reduced or missing in these mutants.

Other genes have been characterized that affect the stability of the PSI complex: *btpA* (Bartsevich and Pakrasi, 1997), *ycf3* and *ycf4* (Boudreau et al., 1997), and *pmgA* (Hihara et al., 1998). These lesions specifically affect the concentration of the PSI complex, with little effect on other photosystems, and therefore may not be a likely explanation for the mutant *hcf*47 phenotype. The *hcf*47 mutant may therefore arise from a general defect similar to the *hcf*106 and *tha1* mutations.

The PSI complex is composed of at least 11 different polypeptides that are believed to be present as one copy

per P700 reaction center (Xu et al., 1995; Chitnis, 1996). In addition, the PSI complex contains approximately 100 chlorophyll *a* molecules, several β-carotene molecules, two phylloquinone molecules, and three [4Fe-4S] clusters. In plants and green algae, PSI is composed of at least 13 different polypeptides and is associated with multiple membrane-embedded light harvesting complexes, which serve as accessory antennas for harvesting light energy and directing it to the PSI reaction center.

The *hcf*44 mutants may have a specific defect in the assembly of functional PSI complexes. The rates of oxygen evolution and uptake were similar for the *hcf*44 mutant and wild-type membranes when using equal amounts of chlorophyll, but were less when calculated on an equal-tissue basis. These data suggest that electron flow through the PSII and PSI reaction centers in the mutant seedlings was intact, but that fewer fully functional reaction centers exist in the mutants. This is supported by the observation that the core PsaA-PsaB complex was present, which may allow initial charge separation in the P700 reaction center to occur. This has been shown in various model systems where specific PSI polypeptides have been deleted without having a significant effect on charge separation (Mannan et al., 1991; Xu et al., 1994; Yu et al., 1995). Although charge separation is able to occur in mutant membranes, the absence of the peripheral PsaD subunit, the Fd-docking polypeptide (Xu et al., 1994), and PsaE, also involved in photoreduction (Rousseau et al., 1993), would prevent Fd-mediated $NADP^+$ photoreduction. Table III shows that $NADP^+$ photoreduction was completely absent in the mutant membranes, suggesting that electron flow may be intact through core subunits but is not sufficient for the reduction of $NADP^+$.

Western analysis showed a specific loss of the PsaC, PsaD, and PsaE subunits from the *hcf*44 mutant membranes. Inactivation of the *psaC* gene product can affect the assembly and function of the PSI complex and specifically the PsaD subunit in many organisms (Mannan et al., 1991, 1994; Takahashi et al., 1991; Yu et al., 1995). Given the absence of PsaD and PsaE from the *hcf*44 mutants, one might suggest a possible defect in the production of the PsaC subunit or its stable integration into the PSI complex. Either situation may exist, since electron flow through the core complex was intact. The absence of a functional PsaC subunit would then explain the absence of the Fd-docking subunit PsaD, since the PsaC subunit is required for the stable integration of PsaD (Yu et al., 1995). The PsaD subunit is also required for the stable assembly of the PsaE subunit (Chitnis and Nelson, 1992), explaining the absence of this subunit in the *hcf*44 mutant membranes.

The *hcf*44 and *hcf*47 mutants have been mapped to the long arm of chromosome 1 (*hcf*44) and the short arm of chromosome 10 (*hcf*47) (Miles et al., 1985). Therefore, a specific lesion in the *psaC* gene, a plastid-encoded gene, is probably not responsible for creating the *hcf*44 mutant. However, *hcf*109, a nuclear photosynthetic mutant of Arabidopsis in which a *trans*-regulatory factor controlling the stability of the *ndhH* operon is suspected of disrupting transcription of the *psaC* gene, has been characterized (Meurer et al., 1996). Other *hcf* mutants of Arabidopsis, such as *hcf*5 (Dinkins et al., 1997), and *hcf*2 (Dinkins et al., 1994), are believed to affect plastid gene expression. There are non-*hcf* genes that affect plastid gene expression as well (Bartsevich and Pakrasi, 1997; Boudreau et al., 1997; Ruf et al., 1997). RT-PCR for the *hcf*44 mutant showed that the level of *psaC* mRNA was similar to that of wild type, suggesting that the transcription of the *psa*C gene was not affected. Therefore, the *hcf*44 mutant represents a lesion in some other nuclear-encoded gene whose gene product specifically affects the synthesis and/or stable integration of the PsaC polypeptide or of the [4Fe-4S] clusters within the PsaC protein.

The loss of photosynthetic capabilities has left the *hcf*44 and *hcf*47 mutants susceptible to light-induced damage. This was especially evident under high light intensity, where mutant seedlings were visually lighter in color, less vigorous, and more susceptible to an earlier death than mutant seedlings grown under medium or low light intensities. Because of the inability of light energy to be dissipated through photochemical quenching, *hcf* mutants may be more susceptible to photooxidative damage. Therefore, the increase in peak fluorescence for mutant seedlings grown under low light intensity may reflect healthier tissue from a reduction in light-induced photooxidative damage compared with seedlings grown under high light intensity.

Much information has been obtained about the process of PSI subunit assembly and function from studying prokaryotic organisms such as S*ynechocystis* sp. PCC 6803. The *hcf*44 mutant of maize was similar to the PsaC-less strain of S*ynechocystis* sp. PCC 6803 and may arise from a defect in the assembly and/or function of the PsaC subunit. RT-PCR showed that this defect occurred beyond the transcription of the plastid *psaC* gene. The *hcf*47 mutant had a more general defect in photosynthesis. Western analysis revealed the deficiency or absence of many PSI and PSII proteins from these membranes, suggesting a general defect in chloroplast membrane biogenesis or the assembly and/or transport of membrane-bound photosynthetic polypeptides. Because of the lack of electron transport, both mutants are susceptible to photooxidative damage under high light stress. Collectively, these observations demonstrate the coordinated assembly of the peripheral proteins into PSI and demonstrate the in vivo requirements of the PsaC, PsaD, and PsaE subunits for the function of PSI in higher plants.

ACKNOWLEDGMENTS

The authors thank John Golbeck, Elena Zak, Himadri Pakrasi, Bridgette Barry, Charles Youcum, and James Guikema for providing many of the antibodies used in this study. The authors also thank Vaishali Chitnis for her expert assistance with the biochemical assays and Michael Hitchler for his enthusiastic technical support, and Wade Johnson and Michael Hitchler for carefully and critically reviewing the manuscript.

Received February 16, 1999; accepted May 5, 1999.

LITERATURE CITED

Ausubel FM, Brent R, Kingston RE, Moore DD, Seidman JG, Smith JA, Struhl K, eds (1988) Current Protocols in Molecular Biology. Wiley-Interscience, New York

Barkan A, Miles D, Taylor WC (1986) Chloroplast gene expression in nuclear, photosynthetic mutants of maize. EMBO J **5:** 1421–1427

Bartsevich VV, Pakrasi HB (1997) Molecular identification of a novel protein that regulates biogenesis of photosystem I, a membrane protein complex. J Biol Chem **272:** 6382–6387

Boudreau E, Takahashi Y, Lemieux C, Turmel M, Rochaix JD (1997) The chloroplast *ycf3* and *ycf4* open reading frames of *Chlamydomonas reinhardtii* are required for the accumulation of the photosystem I complex. EMBO J **20:** 6095–6104

Chitnis PR (1996) Photosystem I. Plant Physiol **111:** 661–669

Chitnis PR (1998) Targeting, assembly and degradation of chloroplast proteins. *In* AS Raghavendra, ed, Photosynthesis: A Comprehensive Treatise. Cambridge University Press, Cambridge, UK, pp 58–71

Chitnis PR, Nelson N (1992) Assembly of two subunits of the cyanobacterial photosystem I on the *n*-side of thylakoid membranes. Plant Physiol **99:** 239–246

Dinkins RD, Bandaranayake H, Baeza L, Griffiths AJ, Green BR (1997) *hcf5*, a nuclear photosynthetic electron transport mutant of *Arabidopsis thaliana* with a pleiotropic effect on chloroplast gene expression. Plant Physiol **113:** 1023–1031

Dinkins RD, Bandaranayake H, Green BR, Griffiths AJ (1994) A nuclear photosynthetic electron transport mutant of *Arabidopsis thaliana* with altered expression of the chloroplast *petA* gene. Curr Genet **25:** 282–288

Gause WC, Adamovicz J (1995) Use of PCR to quantitate relative differences in gene expression. *In* CW Dieffenbach, GS Dveksler, eds, PCR Primer: A Laboratory Manual. Cold Spring Harbor Laboratory Press, Cold Spring Harbor, NY, pp 293–312

He WZ, Malkin R (1992) Specific release of a 9-kDa extrinsic polypeptide of photosystem I from spinach chloroplasts by salt washing. FEBS Lett **308:** 298–300

Hihara Y, Sonoike K, Ikeuchi M (1998) A novel gene, *pmgA*, specifically regulates photosystem stoichiometry in the cyanobacterium *Synechocystis* species PCC 6803 in response to high light. Plant Physiol **117:** 1205–1216

Hipkins MF, Baker NR (1986) Spectroscopy. *In* MF Hipkins, NR Baker, eds, Photosynthesis Energy Transduction: A Practical Approach. IRL Press, Oxford, pp 51–102

Hippler M, Redding K, Rochaix JD (1998) *Chlamydomonas* genetics, a tool for the study of bioenergetic pathways. Biochim Biophys Acta **1367:** 1–62

Mannan RM, Pakrasi HB, Sonoike K (1994) The PsaC protein is necessary for the stable association of the PsaD, PsaE, and PsaL proteins in the photosystem I complex: analysis of a cyanobacterial mutant strain. Arch Biochem Biophys **315:** 68–73

Mannan RM, Whitmarsh J, Nyman P, Pakrasi HB (1991) Directed mutagenesis of an iron-sulfur protein of the photosystem I complex in the filamentous cyanobacterium *Anabaena variabilis* ATCC 29413. Proc Natl Acad Sci USA **88:** 10168–10172

Meurer J, Berger A, Westhoff P (1996) A nuclear mutant of *Arabidopsis* with impaired stability on distinct transcripts of the plastid *psbB*, *psbD/C*, *ndhH*, and *ndhC* operons. Plant Cell **8:** 1193–1207

Miles CD, Daniel DJ (1974) Chloroplast reactions of photosynthetic mutants in *Zea mays*. Plant Physiol **53:** 589–595

Miles D (1980) Mutants of higher plants: maize. *In* A San Pietro, ed, Methods in Enzymology, Vol 69. Academic Press, New York, pp 3–23

Miles D (1994) The role of high chlorophyll fluorescence photosynthesis mutants in the analysis of chloroplast thylakoid membrane assembly and function. Maydica **39:** 35–45

Miles D, Leto KJ, Neuffer MG, Polacco M, Hanks JF, Hunt MA (1985) Chromosome Arm Location of Photosynthesis Mutants in *Zea mays* L. using B-A Translocations. Cold Spring Harbor Laboratory Press, Cold Spring Harbor, NY

Neuffer MG, Coe EH, Wessler SR (1997) Mutants of Maize. Cold Spring Harbor Laboratory Press, Cold Spring Harbor, NY

Pakrasi HB (1995) Genetic analysis of the form and function of photosystem I and photosystem II. Annu Rev Genet **29:** 755–776

Rousseau F, Setif P, Lagoutte B (1993) Evidence for the involvement of PSI-E subunit in the reduction of ferredoxin by photosystem I. EMBO J **12:** 1755–1765

Ruf S, Kossel H, Bock R (1997) Targeted inactivation of a tobacco intron-containing open reading frame reveals a novel chloroplast-encoded photosystem I-related gene. J Cell Biol **139:** 95–102

Settles AM, Yonetani A, Baron A, Bush DR, Cline K, Martienssen R (1997) Sec-independent protein translocation by the maize Hcf106 protein. Science **278:** 1467–1470

Sun J, Ke A, Jin P, Chitnis VP, Chitnis PR (1998) Isolation and functional study of photosystem I subunits in the cyanobacterium *Synechocystis* sp. PCC 6803. Methods Enzymol **297:** 124–139

Takahashi Y, Goldschmidt-Clermont M, Soen S-Y, Franzen LG, Rochaix J-D (1991) Directed chloroplast transformation in *Chlamydomonas reinhardtii*: insertional inactivation of the *psaC* gene encoding the iron sulfur protein destabilizes photosystem I. EMBO J **10:** 2033–2040

Trebst A (1972) Measurement of Hill reactions and photoreduction. *In* A San Pietro, ed, Methods in Enzymology, Vol 24. Academic Press, New York, pp 146–164

Voelker R, Barkan A (1995) Two nuclear mutations disrupt distinct pathways for targeting proteins to the chloroplast thylakoid. EMBO J **14:** 3905–3914

Xu Q, Chitnis VP, Ke A, Chitnis PR (1995) Structural organization of photosystem I. *In* P Mathis, ed, Photosynthesis: From Light to Biosphere. Kluwer Academic Publishers, Dordrecht, The Netherlands, pp 87–90

Xu Q, Jung YS, Chitnis VP, Guikema JA, Golbeck JH, Chitnis PR (1994) Mutational analysis of photosystem I polypeptides in *Synechocystis* sp. PCC 6803: subunit requirements for reduction of $NADP^+$ mediated by ferredoxin and flavodoxin. J Biol Chem **269:** 21512–21518

Yu J, Smart LB, Jung YS, Golbeck J, McIntosh L (1995) Absence of PsaC subunit allows assembly of photosystem I core but prevents the binding of PsaD and PsaE in *Synechocystis* sp. PCC6803. Plant Mol Biol **29:** 331–342